NeuDep: Neural Binary Memory Dependence Analysis

Kexin Pei
kpei@cs.columbia.edu
Columbia University
New York, USA

Dongdong She*
dongdong@cs.columbia.edu
Columbia University
New York, USA

Michael Wang*
mi27950@mit.edu
MIT
Cambridge, USA

Scott Geng*
scott.geng@columbia.edu
Columbia University
New York, USA

Zhou Xuan
xuan1@purdue.edu
Purdue University
West Lafayette, USA

Yaniv David
yaniv.david@columbia.edu
Columbia University
New York, USA

Junfeng Yang
junfeng@cs.columbia.edu
Columbia University
New York, USA

Suman Jana
suman@cs.columbia.edu
Columbia University
New York, USA

Baishakhi Ray
rayb@cs.columbia.edu
Columbia University
New York, USA

ABSTRACT

Determining whether multiple instructions can access the same memory location is a critical task in binary analysis. It is challenging as statically computing precise alias information is undecidable in theory. The problem aggravates at the binary level due to the presence of compiler optimizations and the absence of symbols and types. Existing approaches either produce significant spurious dependencies due to conservative analysis or scale poorly to complex binaries.

We present a new machine-learning-based approach to predict memory dependencies by exploiting the model's learned knowledge about how binary programs execute. Our approach features (i) a self-supervised procedure that pretrains a neural net to reason over binary code and its dynamic value flows through memory addresses, followed by (ii) supervised finetuning to infer the memory dependencies statically. To facilitate efficient learning, we develop dedicated neural architectures to encode the heterogeneous inputs (*i.e.,* code, data values, and memory addresses from traces) with specific modules and fuse them with a composition learning strategy.

We implement our approach in NeuDep and evaluate it on 41 popular software projects compiled by 2 compilers, 4 optimizations, and 4 obfuscation passes. We demonstrate that NeuDep is more precise (1.5×) and faster (3.5×) than the current state-of-the-art. Extensive probing studies on security-critical reverse engineering tasks suggest that NeuDep understands memory access patterns, learns function signatures, and is able to match indirect calls. All these tasks either assist or benefit from inferring memory dependencies. Notably, NeuDep also outperforms the current state-of-the-art on these tasks.

CCS CONCEPTS

• **Security and privacy → Software reverse engineering**; • **Computing methodologies → Machine learning**.

KEYWORDS

Memory Dependence Analysis, Reverse Engineering, Large Language Models, Machine Learning for Program Analysis

ACM Reference Format:
Kexin Pei, Dongdong She, Michael Wang, Scott Geng, Zhou Xuan, Yaniv David, Junfeng Yang, Suman Jana, and Baishakhi Ray. 2022. NeuDep: Neural Binary Memory Dependence Analysis. In *Proceedings of the 30th ACM Joint European Software Engineering Conference and Symposium on the Foundations of Software Engineering (ESEC/FSE '22), November 14–18, 2022, Singapore, Singapore.* ACM, New York, NY, USA, 13 pages. https://doi.org/10.1145/3540250.3549147

1 INTRODUCTION

Binary memory dependence analysis, which determines whether two machine instructions in an executable can access the same memory location, is critical for many security-sensitive tasks, including detecting vulnerabilities [18, 36, 86], analyzing malware [38, 93], hardening binaries [4, 29, 44, 90], and forensics [19, 35, 58, 91]. The key challenge behind memory dependence analysis is that machine instructions often leverage indirect addressing or indirect control-flow transfer (*i.e.,* involving dynamically computed targets) to access the memory. Furthermore, most commercial software is stripped of source-level information such as variables, arguments, types, data structures, etc. Without this information, the problem of memory dependence analysis becomes even harder, forcing the analysis to reason about values flowing through generic registers and memory addresses. Consider the following code snippet where we show two instructions (within the same function) at different program locations. The function is executed twice, resulting in two different traces.

*These authors contributed equally to the paper

ESEC/FSE '22, November 14–18, 2022, Singapore, Singapore

ACM ISBN 978-1-4503-9413-0/22/11…$15.00
https://doi.org/10.1145/3540250.3549147

Address	Instruction	Trace 1	Trace 2
.....			
0x06:	`mov [rax],rbx`*	`rax=0x3;rbx=0x1`	`rax=0x5;rbx=0x1`
.....			
0x1f:	`mov rdi,[0x3]`	`rdi=0x1`	`rdi=0x0`
.....			

*In Intel x86 syntax [77], `mov [rax],rbx` means writing register `rbx` to the memory pointed by register `rax`; [] means dereference a memory address.

The two instructions are memory-dependent (read-after-write) when `rax`=0x3 (Trace 1). When analyzing the code statically, it requires precise value flow analysis to determine what values can flow to `rax` from different program contexts.

Over the last two decades, researchers have made numerous attempts to improve the accuracy and performance of binary memory dependence analysis [5, 6, 11, 16, 22, 34, 71]. The most common approach often involves statically computing and propagating an over-approximated set of values that each register and memory address can contain at each program point using abstract interpretation. For example, a seminal paper by Balakrishnan and Reps on value set analysis (VSA) [5] adopts strided intervals as the abstract domain and propagates the interval bounds for the operands (*e.g.,* registers and memory locations) along each instruction. VSA detects two instructions to be dependent if their intervals intersect. Unfortunately, these static approaches have been shown to be highly imprecise in practice [96]. *Composing* abstract domains along multiple instructions and *merging* them across a large number of paths quickly accumulate prohibitive amounts of over-approximation error. As a result, the computed set of accessed memory addresses by such approaches often ends up covering almost the entire memory space, leading to a large number of false positives (*i.e.,* instructions with no dependencies are incorrectly detected as dependent).

With the advent of data-driven approaches to program analyses [3, 69, 89], state-of-the-art memory dependence analysis is increasingly using statistical or machine learning (ML) based methods to improve the analysis precision [35, 58, 87, 96], but they still suffer from serious limitations. For example, DeepVSA [35] trains a neural network on static code to classify the memory locations accessed by each instruction into a more coarse-grained abstract domain such as stack, heap, and global, and use the predicted memory region to instantiate the value set in VSA. However, such coarse-grained prediction results in high false positives as any two instructions accessing the same region (*e.g.,* stack) will always be detected as dependent even when the instructions access two completely different addresses. To avoid the precision losses by the static approaches, BDA [96] uses a dynamic approach that leverages probabilistic analysis to sample program paths and performs per-path abstract interpretation. However, as real-world programs often have many paths, the cost of performing per-path abstract interpretation for even a smaller subset of paths adds prohibitive runtime overhead, *e.g.,* taking more than 12 hours to finish analyzing a single program. It is perhaps not surprising—while a dynamic approach can be more accurate than static approaches, it can incur extremely high runtime overhead, especially while trying to achieve good code coverage.

To achieve higher accuracy in a reasonably faster time, we propose an ML-based hybrid approach. Our key strategy is to learn to

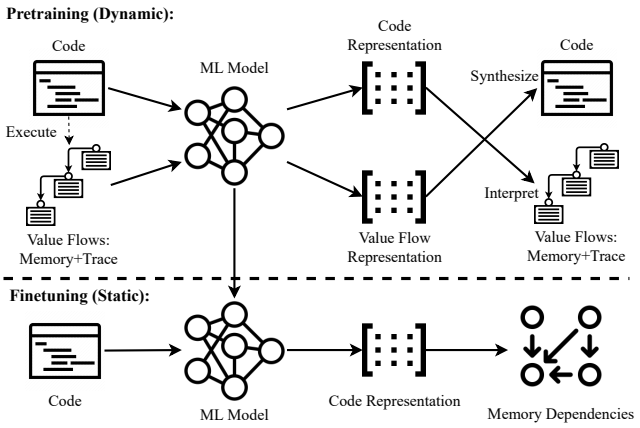

Figure 1: The workflow of our approach. We first pretrain the model to predict code based on its traces and predict traces based on its code. We then finetune the model to statically infer memory dependencies.

reason about approximate memory dependencies from the execution behavior of generic binary code during training. We then apply the learned knowledge to static code during inference without any extra runtime overhead (see Figure 1). Such a hybrid approach, *i.e.,* learning from both code and traces, has been shown promise in several Software Engineering applications, including clone detection, type inference, and program fixing and synthesis [60, 63, 64, 89]. However, none of these works can reason fine-grained value flows through different memory addresses as they do not explicitly model memory. To bridge this gap, we aim to model the memory addresses in the ML-based hybrid framework and try to make fine-grained predictions differentiating the memory contents of different data pointers. Modeling memory address is, however, challenging as it requires the model to (i) distinguish between different memory addresses, (ii) learn to reason about indirect address references and memory contents, and (iii) learn the compositional effects of multiple instructions that involve memory operations.

To this end, we propose a new learning framework comprising pretraining and finetuning steps inspired by masked language model (MLM) [25], as shown in Figure 1. Unlike traditional MLM, where the input is restricted to a single input modality (*e.g.,* text), our model learns from multi-modal information: instructions (static code), traces (dynamic values), and memory addresses (code spatial layout). We deploy a novel fusion module to simultaneously capture the interactions of these modalities for predicting memory dependencies. During pretraining, we mask random tokens from these modalities. While predicting masked opcode teaches the model to *synthesize* the instruction, predicting masked values in traces and memory addresses forces the model to learn to *interpret* instructions and their effect on registers and memory contents. For instance, if we mask the value of `rax` in `mov [rax],rbx` in the above example and train the model to predict it, the model is forced to interpret the previous instructions in the context and reason about how they compute their trace values that flow into `rax`. We hypothesize that

such pretraining helps the model gain a general understanding of the value flow behavior involving memory operations.

After pretraining, the model is finetuned to statically (without the trace values) reason about the value flows (based on its learned knowledge from pretraining) across memory along multiple paths and predict the memory-dependent instruction pairs. Both pretraining and finetuning steps are automated and data-driven without manually defining any propagation rules for value flows. As a result, we show that our model is faster and more precise than the state-of-the-art systems (§5).

We implement our approach in NeuDep by carefully designing a new neural architecture specialized for fine-grained modeling of pointers to distinguish between unique memory addresses (Challenge i). We develop a novel fusion module to facilitate efficient training on the multi-modal bi-directional masking task, which helps the model to understand memory address content and thus, indirect memory references (Challenge ii). Finally, to teach the *compositional effects* of instructions on memory values (Challenge iii), we leverage the principle of curriculum learning [8], *i.e.,* expose short training examples in the initial learning phase, and gradually increase the sample difficulties as the training progresses.

We evaluate NeuDep on a wide range of popular software projects compiled with diverse optimizations and obfuscation passes. We demonstrate that NeuDep is more precise than state-of-the-art binary dependence analysis approaches, widely-used reverse engineering frameworks, and even a source-level pointer analysis tool that has access to much richer program properties. We also show that NeuDep generalizes to unseen binaries, optimizations, and obfuscations, and is drastically faster than existing approaches. We perform extensive ablation studies to justify our design choices over other alternatives studied in previous works [64, 66]. Moreover, NeuDep is surprisingly accurate at many additional security-critical reverse engineering tasks, which either support or benefit from inferring memory dependencies, such as predicting memory-access regions, function signatures, and indirect procedure calls – NeuDep also outperforms the state-of-the-arts on all these tasks.

We make the following contributions:

(1) We propose a new neural architecture that can jointly learn memory value flows from code and the corresponding traces for predicting binary memory dependencies.
(2) We implement our approach in NeuDep that contains a dedicated fusion module for learning encodings of memory addresses/trace values, and a composition learning strategy.
(3) Our experimental results demonstrate that NeuDep is (3.5×) faster and more accurate (1.5×) than the state-of-the-art.
(4) Our extensive ablation studies and analysis on downstream tasks suggest that our pretraining substantially improves the prediction performance and helps the model to learn value flow through different instructions.

2 OVERVIEW

2.1 Motivating Example

Figure 2 shows that two instructions I_2: `mov rdi,[rax+0x8]` and I_7: `mov [rbp+rbx],rdi` access the same memory location (and are thus memory-dependent) but via different addressing registers. To detect the dependency, the model needs to first understand that

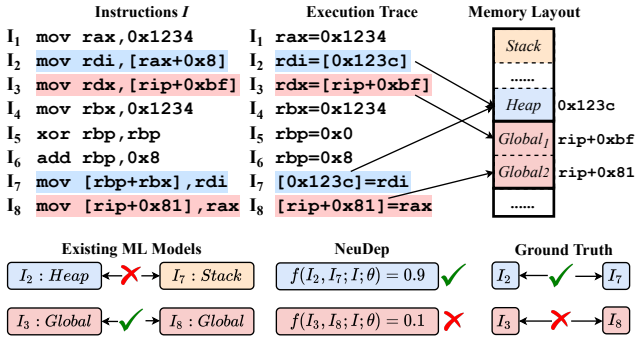

Figure 2: Motivating example of predicting memory dependencies in the function `ngx_init_setproctitle` from `nginx-1.21.1`. I_2 and I_7 access the same heap variable (in blue); I_3 and I_8 access *different* global variables (in red). We find that existing ML-based approaches (learned on static code only) fail to detect I_2 and I_7 are dependent by predicting they access to different memory regions and cannot distinguish the memory accessed by I_3 and I_8 due to the prediction granularity.

the behavior of `mov`: both line 1 (I_1) and line 4 (I_4) set `rax` and `rbx` to the same value. It then needs to understand `xor` in line 5 sets `rbp` to 0, and `add` in line 6 performs addition and sets `rbp` to `0x8`. Finally, the model needs to compose these facts and concludes that `rax+0x8` is semantically equivalent to `rbp+rbx` in such a context, *i.e.,* they both evaluate to `0x123c`.

Gap in Existing Solutions. We find that when running the ML model trained only on static code for this task [35], it mispredicts that I_2 and I_7 are not dependent as their memory-access regions (I_2 accesses heap while I_7 is mispredicted to access stack) do not intersect, possibly because its inference depends on the spurious pattern that the stack base pointer `rbp` is used at line 7. Such mispredictions [35] might lead to a false negative by flagging two instructions as accessing non-overlapping memory regions.

Proposed Solution. The above observation underscores the importance of encoding the knowledge about each instruction's contribution to value flows through memory and their compositions as part of the ML model. However, integrating a memory model as part of the encoded knowledge is challenging due to the presence of potentially complex flows involving indirect address references and their compositions. We address these challenges by designing

(1) A novel training objectives to distinguish between unique memory addresses (§2.2)
(2) A dedicated fusion module sepcialized to capture the interaction between instruction, trace, and memory addresses (§2.3.2). Our new tracing and sampling strategies (§2.3.1) help the ML model to learn value flows across memory addresses.
(3) Curriculum learning [8] in the training process to incrementally learn the compositional effects (§2.3.3).

Table 1 shows some examples of how the pretraining task works and how it teaches the model to reason about value flows.

Table 1: Examples of masking (in grey) instructions and traces (represented as input (In) and output (Out) of each instruction). The model has to dereference the memory content and interpret or synthesize instruction(s) to infer the masked parts. We include the actual operations performed by the instructions (noted in green) and the formal semantics that the model essentially needs to learn for each example (last column).

Example Descriptions	Instruction(s) Mnemonic	Operand	Trace In	Trace Out	Underlying Semantics
Example 1: *Interpreting* memory operands in bitwise operations Let the output value of `rax` in `xor rax,[rbx]` be masked. To predict the masked value (*i.e.,* `rax`=0x2), the model needs to understand the semantics of `xor` on its inputs `rax`=0x2 and `[rbx]`=0x7.	`rax=rax⊕[rbx]`				
	`xor`	`rax`	0x2	**0x5**	$v_1 = 0x2, v_2 = 0x7$
		`[rbx]`	0x7	0x7	$v = v_1 \oplus v_2$ / $v = 0x5$
Example 2: *Synthesizing* Arithmetic Operations with memory operands Let `add` be masked in `add rbp,[rdi]`. To predict the masked `add` (*e.g.,* out of `sub`, `mov`, etc.), the model needs to associate `add` to the behavior that increments the its first operand by that of its second operand.	`rbp=rbp+[rdi]`				
	`add`	`rbp`	0x4	0xc	$v_1 = 0x4, v_2 = 0x8$
		`[rdi]`	0x8	0x8	$v = v_1 \diamond v_2, v = 0xc$ / $\diamond$ = `add`
Example 3: Reverse *Interpreting* Arithmetic Operations with memory operands Let the input value of `rcx` in `sub rcx,[rdx]` be masked. To predict the masked value, the model needs to interpret `sub` *backward* given its output 0x8 and the value of its second operand 0x1 stored on memory.	`rcx=rcx-[rdx]`				
	`sub`	`rcx`	**0x9**	0x8	$v_2 = 0x1, v = 0x8$
		`[rdx]`	0x1	0x1	$v = v_1 - v_2$ / $v_1 = 0x9$

Example 4: *Interpreting Compositions* of Multiple Memory Operations
More than one instructions are executing. Let the output value of `rsi` in `push rdi;mov rsi,[rsp]` be masked. To predict the masked value, the model needs to first interpret `push` and understand its side effect: decrements the stack pointer `rsp` by 8 bytes and store the value of `rdi` (0x6) on stack referenced by `rsp`.
The model then needs to first dereference the indirect addressing of `[rsp]` to infer 0x6 is stored at `rsp` (0x0). It then needs to interpret `mov` and understand it assigns the value from its second operand to the first operand to infer the masked value to be 0x6.
	`rsp=rsp-0x8`
	`[rsp]=rdi`
	`rsi=[rsp]`			

	`push`	`rdi`	0x6	0x6	$v_1 = v_1 - 0x8$
		`rsp`	0x8	0x0	$[v_1] = 0x6$
	`mov`	`rsi`	0x0	**0x6**	$v_2 = [v_1]$ / $v_2 = 0x6$
		`[rsp]`	0x0	0x0	

2.2 Problem Formulation

Let f denote an ML model parameterized by θ. Before directly training f towards predicting memory dependencies, we pretrain f to reason about the value flows (see §3.4 for details). Now consider f with pretrained parameters θ, we formalize the task of analyzing memory dependencies as follows.

Definition 2.1 (Memory Dependency Prediction)**.** Given a pair of assembly code instructions $\{I_i, I_j\}$ within a code block I consisting of n assembly instructions: $(I_1, ..., I_n)$, our neural memory dependency predictor f, parameterized by the pretrained weight θ, predicts whether the instruction pair can access the same memory location, *i.e.,* $y = f(I_i, I_j, I; \theta), y \in [0, 1]$. $y = 0$ denotes $\{I_i, I_j\}$ do not have memory dependency, and $y = 1$ denotes dependent.

Any y between 0 and 1 denotes the probability of I_i and I_j being dependent. Figure 2 shows an example how our model predicts different instruction pairs. We elaborate on how our neural architecture implements f in the above definition in §3.5.

2.3 NeuDep's Design

Training the model to learn value flows for memory dependence analysis opens up several interesting design spaces, ranging from tracing to introduce diverse behaviors to designing appropriate inductive biases in the model architecture and training strategies. We overview our design in the following and provide detailed descriptions in §3.

2.3.1 Trace Collection. Pretraining requires high-quality training data to expose *diverse* program execution. We implement a forced execution engine [30, 67] to execute individual functions with full path coverage without the reliance on program test cases. Our execution engine differs from the existing works in two key aspects.

First, we note that existing works [28, 66, 67] implement the forced execution by violating the control flow semantics, *i.e.,* stepping through control transfer instructions, to obtain traces with high coverage. However, this introduces noisy traces as they are not realizable in practice. On the contrary, respecting control transfers [64] will inevitably suffer from the coverage problem, as they have to find test cases to cover different paths [12, 20, 59]. To circumvent this problem, we implement a *coverage-guided semantic-preserving* branch-flipping mechanism to expose diverse paths within the function without breaking the branching instructions' semantics (§3.1).

Second, existing works do not trace behaviors of the external procedure calls [64, 66], but this is especially important to model memory operations as heap allocation is often performed via library calls (*e.g.,* via `malloc`). Our tracing engine provides complete environment support by pre-loading the whole program and its dependent libraries. The side effect of all function call instructions can thus be traced and logged as their input-output behavior (§3.1).

2.3.2 Representing and Fusing Code, Trace, and Memory. Assembly instructions and their traces are highly heterogeneous, *i.e.,* instruction consists of discrete tokens like mnemonics and operands, while trace consists of mostly continuous values. To better encode the nature of each sequence, we employ two distinct modules to learn on these two inputs and then fuse them to make the joint inference. Specifically, we learn the instruction sequence with self-attention layers [83] to encode the instructions grounded on their neighboring context. We learn the trace values by a per-byte convolution network. After learning a basic representation of the code and trace values, we employ a fusion module (§3.3) to augment the contextualized instruction embeddings with the trace value embeddings.

We represent the code address space during execution as an additional input aligned to the instructions. This helps the model stay

aware of the instructions' order to their execution effect. Moreover, we observe that **rip**-relative addressing is frequently used to access global variables in position-independent code. Therefore, feeding addresses can help the model to learn the semantics of memory addressing. For example, consider the following instructions from the function `quotearg_free` in `runcon` from Coreutils-8.30.

```
0x449c:   cmp [rip+0x4d65],2          # rip+0x4d65=0x9208
.....
0x44bc:   movsxd rax,[rip+0x4d45]     # rip+0x4d45=0x9208
.....
0x450e:   mov [rip+0x4cf0],1          # rip+0x4cf0=0x9208
```

Three instructions use **rip** with different offsets to access the same global variable stored at `0x9208`. By encoding the address of each instruction, we help the model infer the value of **rip** and thus assist reasoning of the memory dependencies.

2.3.3 Training Design (Composition Learning). Inspired by how humans learn, we aim to develop a strategy that trains the model to gradually build up its knowledge. Ideally, the model should start by learning easy samples and then generalize its learned knowledge by getting exposed to more challenging training samples. As demonstrated in Table 1, the training samples with more instructions are more challenging to predict than those with fewer instructions, as the model has to learn the *compositional* execution effect of multiple instructions. Moreover, the more masks applied, the less context the model can leverage to make the prediction, thus increasing difficulty. Therefore, we develop a curriculum learning strategy [8] by sorting the training samples based on their length and increasing the masking rate at each training epoch. As a result, the model always starts learning from short code pieces with fewer masks at the early batches within each epoch, and the length of the code piece and the number of masks applied are increased in later epochs.

2.4 Additional Reverse Engineering Tasks

To explore how exactly pretraining helps analyze memory dependencies, we investigate what knowledge or properties of programs the pretrained model learns. We resort to *probing*, which uses the encoded instruction representations of the pretrained model and finetunes them on the probing tasks, usually with a small number of labeled data and training epochs [54]. Specifically, we consider three critical reverse engineering tasks, which either assist or benefit from analyzing memory dependencies. If the pretrained model performs well on these reverse engineering (*i.e.,* probing) tasks, it gives evidence that pretraining has encoded useful representation for analyzing memory dependencies.

Inferring Memory Regions. Inferring memory-access regions helps reduce the spurious dependencies reported by VSA (§1). We consider the task sketched in DeepVSA [35], where the model needs to statically predict the memory region accessed by each instruction that operates on memory.

Definition 2.2 (Memory Region Prediction)**.** Given a code block consisting of a sequence of n assembly instructions: $I = (I_1, ..., I_n)$, a memory region predictor f_r, parameterized by the pretrained weights θ, predicts the memory region accessed by each instruction: $y = f_r(I; \theta), y \in \mathbb{M}^n, \mathbb{M} = \{\texttt{stack}, \texttt{heap}, \texttt{global}, \texttt{other}\}$.

Inferring Function Signature. Traditionally, function signatures are predicted by analyzing the memory access patterns of variables and propagating the types implied by the inferred patterns up to the function argument. Memory dependencies help the propagating types along the dependent instructions [49]. The inferred variable types, in turn, also help reduce the spurious bogus dependencies, *i.e.,* two memory accesses with different types are not dependent. We consider the task described in EKLAVYA [15], where the model statically predicts the function signature, including the (i) argument arity, (ii) argument types, and (iii) function return types.

Definition 2.3 (Function Signature Prediction)**.** Given an n-instruction procedure P: $P = (I_1, ..., I_n)$, a function signature predictor f_s, parameterized by the pretrained weights θ, predicts the function signature as follows. (i) When P is treated as callee, f_s predicts P's signature: $y = f_s(P; \theta)$. (ii) When P is treated as caller, f_s takes call site $I_c \in P$ as an additional input, and predicts the signature of the procedure that I_c calls: $y = f_s(P, I_c; \theta)$. In both cases, $y = (a, A, r)$ is a tuple where (i) $a \in [0, 7]$ denotes argument arity with at most 7 arguments. (ii) $A = (A_1, A_2, A_3)$ denotes P's first 3 argument types: $A_i \in \{\texttt{int}, \texttt{char}, \texttt{float}, \texttt{ptr}, \texttt{enum}, \texttt{union}, \texttt{struct}\}$. (iii) $r \in \{\texttt{int}, \texttt{char}, \texttt{float}, \texttt{ptr}, \texttt{enum}, \texttt{union}, \texttt{struct}, \texttt{void}\}$ is the procedure P's return type.

Matching Indirect Calls. Analysis of memory dependencies has been extensively applied to infer indirect calls [47, 96]. Therefore, we study how the pretrained model performs on this task.

Definition 2.4 (Matching Indirect Calls)**.** Given a pair of procedures P_i, P_j, an indirect call predictor f_c predicts whether P_i can call P_j during runtime: $y = f_c(P_i, P_j)$, where $y \in \{0, 1\}$; $y = 1$ denotes P_i can call P_j while $y = 0$ denotes P_i cannot.

Unlike the first two tasks, we define f_c as deterministic function that takes as input the inferred function signatures (Definition 2.3) of P_j and the call-site within P_i. f_c outputs 1 if and only if the signature of P_j closely matches at least one call-site signature within P_i. We elaborate on the matching criteria in §3.6.

3 METHODOLOGY

This section elaborates on the design of NeuDep, including the tracing framework, the model's input representation, the neural architecture, and the training tasks.

3.1 Tracing Framework

Algorithm 1 shows how our tracing framework works on a procedure. We consider the following two key designs (§2.3).

Environment Support. As shown in Algorithm 1 line 1 and 2, we first load the entire binary into an emulator and make a snapshot of the process image after initializing all dependent libraries. We then iterate every function inside the binary and execute each function (line 4 and 5). Before the execution, we restore the process memory using the saved snapshot (line 6) to ensure that all the functions, including external library functions, are properly resolved.

Branch Flipping. Inspired by coverage-guided fuzzing, we design a dynamic branch flipping mechanism for recording complete and diverse execution behaviors. We first maintain a list of covered basic blocks during past execution (line 8-15). We then hook every conditional branch during forced execution and monitor the jump target. If the jump target has already been covered before and another is not covered yet, we flip the branch. In order to ensure

Algorithm 1 Coverage-Guided Semantic-Preserving Execution

```
Load(binary)                                   ▷ Load binary into emulator
mem = Snapshot()                               ▷ Save memory snapshot after initialization
covered_bb = {}
for func ∈ binary do                           ▷ Loop every function
    Restore(mem)                               ▷ Restore memory snapshot
    Initialize(stack, regs)                    ▷ Initialize stack and registers with random values
    /* Loop every conditional branch */
    for cond_branch ∈ ForceExec(func) do
        /* bb1, bb2 are jump targets, bb1 is the default one */
        if bb1 ∈ covered_bb and bb2 ∉ covered_bb then
            FlipBranch(cond_branch)
            covered_bb.add(bb2)
        else
            covered_bb.add(bb1)
```

the flipped branch does not introduce violations of instruction semantics, we implement a semantic-preserving mechanism by patching branch instructions with reverse conditions if it is flipped. For example, a flipped branch instruction `je 0x8a` will be patched to `jne 0x8a`.

3.2 Input Representation

At a high level, NeuDep takes three sequences as input, *i.e.,* assembly instructions, trace values, and instruction addresses.

Assembly. We represent the assembly instructions $I = (I_1, ..., I_n)$ as n ordered tuples. Each tuple I_i consists of 3 members: $I_i = (c_i, p_i, m_i)$, where c_i, p_i, m_i indicate code token, position, and whether c_i accesses memory, respectively. Specifically, c_i denotes the tokens obtained from tokenizing the assembly instructions, removing punctuations, and transforming all constants to `const`. As we flatten each instruction to multiple tokens, we use p_i to annotate the relative position of c_i within the instruction to specify the instruction boundary. Moreover, p_i helps the self-attention layers, which are permutation-invariant to the input tokens, to understand the relative order of the operands. Finally, $m_i \in \{F, T\}$ denotes whether c_i accesses memory.

Example 3.1. Consider the instruction sequence `add rax,0x8;mov [rax],rbx`. It will be represented as:

I	I_1	I_2	I_3	I_4	I_5	I_6
c	add	rax	const	mov	rax	rbx
p	1	2	3	1	2	3
m	F	F	F	F	T	F

Trace. We represent the trace values using $T = (T_1, ..., T_n)$ aligned to the assembly instruction sequence I. Each $T_i \in T$ consists of a list $T_i = (b_1^i, ..., b_8^i)$, where the numeric value is a (padded) 8-byte values $b^i_{j\in[1,8]}$. This reduces a prohibitively large vocabulary (2^{64}) to a much more manageable size (256) [64]. The most and least significant byte is b_1 and b_8, respectively. We further normalize each byte $b^i_{j\in[1,8]}$ into $[0, 1)$ to stablize the training. For instruction tuples I_i whose c_i is not a register or a constant, its aligned trace values T_i contains 8 dummy values (-), which will not be masked during pretraining (§3.4). For T_i whose aligned I_i is not executed, we assign the value b_j =`0x100`, $\forall j \in [1, 8]$. In pretraining, to predict the trace value consisting of all 100s instead of regular bytes, the model needs to determine whether the corresponding assembly instructions are executed by reasoning the branch predicate and control flow.

Example 3.2. Consider the following 4 instructions: `add rax,0x8;cmp rax,0x10;je 0x1004a8b5f;push rdi`; input `rax`=`0x0`. T will look like (aligned with c_i):

c	add	rax	const	cmp	rax	const	je	const	push	rdi
T	T_1	T_2	T_3	T_4	T_5	T_6	T_7	T_8	T_9	T^*_{10}
b_1	-	00	00	-	00	00	-	00	-	100*
b_2	-	00	00	-	00	00	-	00	-	100*
b_3	-	00	00	-	00	00	-	00	-	100*
b_4	-	00	00	-	00	00	-	01	-	100*
b_5	-	00	00	-	00	00	-	00	-	100*
b_6	-	00	00	-	00	00	-	4a	-	100*
b_7	-	00	00	-	00	00	-	8b	-	100*
b_8	-	00	08	-	08	10	-	5f	-	100*

*We show the byte value before normalization to save space. As T_{10} corresponds to `rdi`, which is not executed, its value is 1, which is `0x100` before normalizing.

Address. Similar to trace value sequence T, we represent the address of each instruction (when loaded in memory) as n ordered lists, $A = (A_1, ..., A_n)$, aligned to I. $A_i \in A$ consists of 8 bytes organized as an ordered list: $A_i = (b_1^i, b_2^i, ..., b_8^i)$. On a 64-bit architecture, 8 bytes are enough to represent all possible virtual addresses of a running program. For c_i within one instruction (*e.g.,* Example 3.1), they share the same instruction address.

Example 3.3. Consider 2 instructions: `push rbp;jmp rax` start from the address `0x14a8b`. A will look like (aligned with c_i):

c	push	rbp	jmp	rax
A	A_1	A_2	A_3	A_4
b_6	01	01	01	01
b_7	4a	4a	4a	4a
b_8	8b	8b	8c	8c

We omit showing $b_1, ..., b_5$ as they are all zeros

As the machine instruction of `push rbp` only takes one byte (`0x55`), the addresses of two instructions are off by one byte.

3.3 NeuDep Architecture

Figure 3 illustrates NeuDep's architecture. In the following, we describe how the inputs (§3.2) are embedded, fused, and further processed to make the prediction. All these steps are handled by neural modules that can be stacked together and trained end-to-end.

Input Embeddings. Let d denote the embedding dimension, we denote the embeddings of each tuple (c_i, p_i, m_i) as $E(c_i), E(p_i), E(m_i) \in \mathbb{R}^d$. We sum these embeddings to form the embeddings of I_i: $E(I_i) = E(c_i) + E(p_i) + E(m_i)$. We denote the embedding of all tokens as $E^0(I) = (E(I_1), ..., E(I_n))$, representing the instructions' embeddings before the first self-attention layer. We first apply l self-attention layers on $E^0(I)$ to learn the contextual embeddings of the assembly instructions: $E^l(I)$.

To embed the 8-byte values in T and A into a space that preserves their numerical properties, we employ a convolution network with 8 kernels to learn how bytes within each neighboring size interact with each other. Let C_w denote applying a convolution filter with width w and output channel O_w, we first apply 8 convolution filters on $T_i = (b_1, ..., b_8)$ and concatenate them: $C_{out} = concat(\phi(max(C_1(T_i))), ..., \phi(max(C_8(T_i))))$. Here ϕ denotes an activation function, and we use ReLU in this paper.

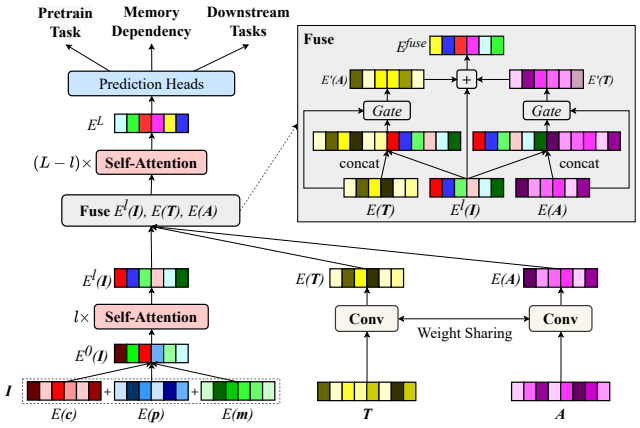

Figure 3: NeuDep's high-level architecture with details of the fusion module. It takes as input 3 sequences: the instructions I, trace values T, and code addresses A (§3.2), where I is embedded by l self-attention layers, and T and A are embedded by convolution networks. They are then fused by a fusion module. The fused embeddings go through another $L-l$ self-attention layers and output the final embeddings E^L (§3.3).

$C_{out} \in \mathbb{R}^{\sum_{w=1}^{8} O_w}$ is the concatenated result. We then transform C_{out} by a highway network [76] (see Appendix) and obtain the embedding for T_i: $E(T_i)$.

To learn a universal value representation from 8 bytes, we share the weights of this network by applying it on both T and A. Therefore, $E(A_i)$ is embedded similarly as described above.

Fusing Heterogenous Inputs. Intuitively, after embedding all the inputs, they are expected to carry basic meaning in their own modalities. We then employ a fusion module that augments the instruction embedding by its traces and address. Specifically, let $G_{T_i} = \sigma(MLP(concat(E^l(I_i), E(T_i))))$ and $G_{A_i} = \sigma(MLP(concat(E^l(I_i), E(A_i))))$ denote the learned gates that control how much $E(T_i)$ and $E(A_i)$ should be fused in $E^l(I_i)$, we have:

$$E_i^{fuse} = E^l(I_i) + G_{T_i} \cdot MLP(E(T_i)) + G_{A_i} \cdot MLP(E(A_i))$$

Cross-Modality Inference. Let L denote the total number of self-attention layers, in which l-th layers are used to learn the instruction representation $E^l(I)$. We feed $E^{fuse} = (E_1^{fuse}, ..., E_n^{fuse})$ to the remaining $L-l$ layers. On top of the last self-attention layer, we obtain $E^L = (E_1^L, ..., E_n^L)$ and employ trainable prediction heads for pretraining (§3.4), finetuning (§3.5), and probing (§3.6).

3.4 Pretraining: Interpret and Synthesize Code

We give the formal definition of our pretraining task as follows.

Definition 3.1 (Pretraining). Given (i) a code block $I = (I_1, ..., I_n)$, (ii) its trace T: $T = (T_1, ..., T_n)$, and (iii) a mask rate r, we pretrain the model f, parameterized by θ, by the following training objectives.

(1) *Interpret* I: predict the masked trace T_{MT}: $T_{MT} \subseteq T, |T_{MT}| = |T| \cdot r$, given I and $T - T_{MT}$: $T_{MT} = f(I, T - T_{MT}; \theta)$.
(2) *Synthesize* I: predict the masked instructions I_{MI}: $I_{MI} \subseteq I, |I_{MI}| = |I| \cdot r$, given $I - I_{MI}$ and T: $I_{MI} = f(I - I_{MI}, T; \theta)$.
(3) *Both*: predict both I_{MI} and T_{MT} given $I - I_{MI}$ and $T - T_{MT}$: $I_{MI}, T_{MT} = f(I - I_{MI}, T - T_{MT}; \theta)$.

Specifically, the pretraining takes as input the output of the last self-attention layer $E^L = (E_1^L, ..., E_n^L)$, and minimize the (1) cross-entropy (CE) between the predicted masked code $\hat{c}$ and the actual code c_{MI}, and the (2) mean squared error (MSE) between predicted masked values (8 bytes) $\hat{T}_{MT}$ and the actual values T_{MT}:

$$\arg\min_{\theta} \sum_{i \in MI} -c_i \log(\hat{c}_i) + \alpha \sum_{j \in MT} (\hat{T}_j - T_j)^2 \quad (1)$$

θ denote the trainable parameters NeuDep's model (§3.3) and the prediction heads: MLP_c and MLP_T, two multilayer perceptrons that take E^L as input and predict the masked instructions: $\hat{c}_{MI} = MLP_c(E_{MI}^L)$ and trace values: $\hat{T}_{MT} = MLP_T(E_{MT}^L)$.

Composition Learning. We increase the masking percentage r (Definition 3.1) at each epoch. Let L, U denote the lower and upper bound of the r, respectively, and $EPO_{pretrain}$ denote the pretraining epochs, at k-th epoch, $r = L + (U - L) \times (k-1)/EPO_{pretrain}$.

3.5 Finetuning: Predict Memory Dependencies

As shown in Figure 1, after the model is pretrained, we let the model predict value flows between instructions based on its learned representation of assembly code without traces. To this end, we detach the fusion module and the convolution module for embedding the trace T and addresses A (right part in Figure 3) and directly stack the upper $L-l$ self-attentions on top of the first l self-attention layers.

Given $E^L = (E_1^L, ..., E_n^L)$ (§3.3), we employ a prediction head MLP_{dep} that minimizes the binary cross-entropy (BCE) between the predicted dependency $\hat{y}$ of $\{I_i, I_j\} \subseteq I$ and their ground truth y (Definition 2.1): $\arg\min_\theta -y \cdot \log \hat{y} - (1-y) \cdot \log(1-\hat{y})$, where

$$\hat{y} = MLP_{dep}(concat(\psi_a(E^L), E_i^L, E_j^L, |E_i^L - E_j^L|, E_i^L \odot E_j^L))$$

Here ψ_a denotes taking the mean pooling of E^L and $\odot$ denotes element-wise multiplication. This results in the input shape to MLP_{dep} to be $\mathbb{R}^{5d}$.

3.6 Downstream Reverse Engineering Tasks

As described in §2.4, we consider three security-critical reverse engineering tasks as our probing tasks. We follow the similar setup in §3.5 and stack separate prediction heads on top of E^L, and train with additional training samples collected for probing.

Inferring Memory Regions. Given the output of the last self-attention layers $E^L = (E_1^L, ..., E_n^L)$, we stack a prediction head MLP_r that predicts the memory-access regions for each instruction I_i. The training task then minimizes the sum of cross-entropy between the predicted memory regions $\hat{y}$ of *each* instruction and their ground truth memory region y: $\arg\min_\theta \sum_{i=1}^n -y_i \cdot \log(MLP_r(E_i^L))$.

Inferring Function Signature. As shown in Definition 2.3, predicting function signatures consists of predicting 5 types of labels: $\{a, A_1, A_2, A_3, r\}$. For each label, we create two prediction heads: MLP_{caller} and MLP_{callee}. For example, MLP_{caller}^a takes as input the embedding corresponding to the call site $c \in [1, n]$ from the last

self-attention layer E^L, and predicts the number of arguments that the call site prepares: $a = MLP^a_{caller}(E^L_c)$. MLP^a_{callee} takes as input the embeddings from the last self-attention layer E^L and predicts the number of arguments the callee expects: $a = MLP^a_{callee}(\psi_a(E^L))$ where ψ_a denotes the average pooling of all embeddings in E^L. The training objective for each head then minimizes the cross-entropy loss between the predicted label and the ground truth label.

Matching Indirect Calls. Given the signatures of a call site P_i and a callee P_j, we implement the indirect call predictor f_c (Definition 2.4) by considering the following 4 criteria. (i) *Loose arity*: P_i must prepare at least as many arguments as P_j accepts. (ii) *Strict arity*: the arities of P_i, P_j must match exactly. (iii) *Argument type*: the types of P_i's first three arguments must match P_j's argument types in at least 2 or 3 positions. (iv) *Return type*: if P_i is non-void, then P_j must be non-void. The four criteria can be composed to determine whether P_i, P_j matches. We evaluate the 8 compositions in §5.3.

4 IMPLEMENTATION AND SETUP

We implement NeuDep's tracing framework in Qiling [81] and the model architecture based on PyTorch. We run all experiments and baselines on a Linux server, with Intel Xeon 4214 at 2.20GHz with 48 virtual cores, 188GB RAM, and 4 Nvidia RTX 2080Ti GPUs.

Dataset. We collect 41 open-source projects, ranging from utility libraries like Binutils to popular libraries like OpenSSL (see Appendix). We compiled these projects with 4 optimizations, *i.e.,* O0-O3, using GCC-9.3.0, and 4 obfuscations based on Clang-8 [94], *i.e.,* bogus control flow (bcf), control flow flattening (cff), basic block splitting (spl), and instruction substitution (sub). Among the 41 projects, we select 9 projects as our finetuning set and the rest for pretraining. They include bash-5.0, bc-1.07.1, binutis-2.30, bison-3.3.2, cflow-1.6, coreutils-8.30, curl-7.76.0, findutils-4.7.0, gawk-5.1.0. The 9 projects have disparate functionalities and sizes such that they are diverse and representative of real-world software. We perform static disassembly (taking less than 0.1 seconds per input) followed by a simply post-processing to parse the raw assembly into the format that the model accepts (§3.2).

Ground Truth Dependencies. We follow [96] by using dynamic analysis to collect the ground truth memory dependencies. To quantify how NeuDep and the baselines perform, we measure the detected dependencies among the reference ones (*detect*) and mark the rest as *miss*; we treat the predicted dependencies not included in the references as potential false positives (FP).

Baselines. We compare NeuDep to Angr [85], Ghidra [1], SVF [78], and DeepVSA [35]. As SVF does support dumping its result to the compiled binary (confirmed with the authors) [78], we propagate its result using the DWARF information. As one source statement can map to multiple assembly instructions, we treat it as a true positive if its detected dependencies include the ground truth instruction pair. We thus omit evaluating SVF on the obfuscated binaries as the obfuscator significantly distorts the mapping in DWARF. For DeepVSA, its VSA implementation requires taking a crash dump as input and does not work for general memory dependence analysis. Therefore, we run its released trained model and use its predicted memory region to determine whether two memory-access instructions are dependent. We note that PalmTree [51] also compared to DeepVSA on the standalone memory region prediction task without running its VSA module. However, as PalmTree does not release its trained model for memory region prediction, we cannot run PalmTree on our dataset to predict memory dependencies. Therefore, we instead compare NeuDep to PalmTree and its evaluated baselines (including DeepVSA) in our probing studies (5.3).

BDA [96] is the state-of-the-art binary memory dependence analysis tool, to the best of our knowledge. We reached out to the authors and confirmed that BDA targets reducing false negatives in the inter-procedural setting, and they evaluated it on only O0 binaries. Per our requests, BDA authors performed preliminary studies and observed BDA achieves low miss rate (0.02%), but suffers from high false positive rate and runtime overhead. For example, on readelf compiled by O0, BDA has around 2.23% precision (detecting 5,742 true dependencies out of a total of 256,596 predicted dependencies). Due to the different focuses between BDA and NeuDep, we thus omit including BDA results to avoid unfair comparison.

For probing tasks, we compare NeuDep to (i) PalmTree [51] and the other baselines that PalmTree evaluated such as DeepVSA [35], Asm2Vec [27], and Instruction2Vec [50], on predicting memory-access regions, (ii) EKLAVYA [15] on predicting function signatures, and (iii) EKLAVYA and TypeArmor [82] on predicting indirect calls.

Hyperparameters. For composition learning, we set $L = 0.2$ and $U = 0.8$ (§3.4). For pretraining (Equation 1), we set $\alpha = 100$ by observing that MSE loss is around 100× smaller than that of CE in our experiments.

5 EVALUATION

We focus on three main research questions in the evaluation.

- **RQ1:** How well does NeuDep perform in analyzing memory dependencies? (§5.1)
- **RQ2:** How much does each design choice in NeuDep contribute to its performance? (§5.2)
- **RQ3:** How well does NeuDep perform in downstream reverse engineering tasks? (§5.3)

5.1 NeuDep Performance

Table 2 presents the results of NeuDep and other baselines on the test set categorized by their optimization and obfuscation flags. NeuDep's results are obtained from finetuning a single model on all datasets, excluding the testing set. On average, NeuDep detects 1.5× more dependencies than the second-best (DeepVSA), while having 4.5× fewer misses than the second-best (SVF). Ghidra has fewer false positives than NeuDep, but at the cost of missing substantial dependencies, detecting 3.3× fewer dependencies than NeuDep. Besides, we note that DeepVSA produces 6.4× more false positives on higher optimizations when compared to O0. This is likely because memory access patterns (*e.g.,* using `rbp` and `rax` to access stack and heap, respectively, are largely broken by compilers.

Zero-Shot Generalizability to Unseen Projects. In the above experiment, our training and testing set are randomly sampled with non-overlapping pairs, but they could come from the same software project. Therefore, we investigate how NeuDep performs when its testing set comes from entirely different software projects. We collect 2 software projects featuring a web server, *i.e.,* Nginx-1.21.1,

Table 2: NeuDep and other baselines' results on the test set categorized by the compiler optimizations and obfuscations.

Flags	# Dep	Angr			Ghidra			SVF			DeepVSA*			NeuDep		
		Detect	Miss	FP	Detect	Miss	FP	Detect	Miss	FP	Detect	Miss	FP	Detect	Miss	FP
O0	1,013	28	985	16	355	658	7	380	633	392	420	593	329	**930**	**83**	**147**
O1	1,310	12	1,298	14	387	923	19	486	824	1,474	617	693	2,013	**898**	**412**	**576**
O2	1,103	14	1,089	10	330	773	6	403	698	1,392	464	639	1,512	**822**	**281**	**480**
O3	1,132	14	1,118	14	332	800	14	425	707	1,351	472	660	1,527	**827**	**305**	**501**
bcf	3,144	23	3,121	14	160	2,984	0	-	-	-	613	2,531	445	**3,122**	**22**	**127**
cff	758	22	736	9	208	550	0	-	-	-	337	421	113	**724**	**34**	**56**
spl	1,296	24	1,272	18	173	1,123	2	-	-	-	515	781	181	**1,245**	**51**	**77**
sub	938	22	916	14	264	674	7	-	-	-	393	545	236	**885**	**53**	**127**
Avg.	1,337	20	1,317	14	276	1,061	7	424	716	1,152	478	858	795	**1,182**	**155**	**261**

*DeepVSA's VSA implementation takes crash dumps as input and does not work on our dataset (regular binary code without crashes). Therefore, we run DeepVSA's released model on our dataset and use its predicted memory region to flag dependent instructions (§4).

Table 3: NeuDep performance when dividing its dataset by non-overlapping train-test vs. non-overlapping programs, optimizations, and obfuscations. Δ denotes the performance change scaled by the number of reference dependencies.

Cross-		# Dep	Regular		Unseen		Δ (+/-)	
			Detect	FP	Detect	FP	Detect	FP
Proj.	Nginx	226	164	56	155	68	-4%	+5.3%
	Lynx	322	240	92	244	120	+1.2%	+8.7%
Opt.	O0	1,013	959	90	958	103	-0.1%	+1.3%
	O1	1,310	1,026	112	988	298	-2.9%	+14.2%
	O2	1,103	919	195	908	208	-1%	+1.2%
	O3	1,132	922	207	933	235	+1%	+2.5%
Obf.	bcf	3,144	3,131	104	2,946	925	-5.9%	+26.1%
	cff	758	746	38	748	35	+0.3%	-0.4%
	spl	2,217	2,171	121	2,076	101	-4.3%	-0.9%
	sub	938	907	76	914	89	+0.8%	+1.4%
Avg.		1,216	1,119	109	1,087	218	-2.6%	+9%

Table 4: Runtime of NeuDep vs. Angr and Ghidra. The last column shows the speedup over the second-best tool.

	Size (MB)	Inference Time (s)			Speedup
		Angr	Ghidra	NeuDep	
bash	2.8	7685.9	60.4	**24.4**	**2.5×**
bc	0.5	298.8	5.3	**1.4**	**3.8×**
binutils	74	70157.1	3077.2	**695.6**	**4.4×**
bison	1.6	1730.1	30.2	**10.3**	**2.9×**
cflow	0.56	695.9	6.5	**3**	**2.2×**
coreutils	16	40,188.2	392.2	**105.9**	**3.7×**
curl	0.77	91.5	14.5	**3.1**	**4.7×**
findutils	2.3	882.7	80.1	**23.2**	**3.5×**
gawk	3.8	2305.3	55.0	**14.1**	**3.9×**
Avg.	12.8	13781.7	413.5	**110.1**	**3.5×**

and a web browser, *i.e.,* Lynx-2.8.9, to which none of the projects in our dataset has similar functionality. We compile each software project with 4 optimizations (O0-O3), and test NeuDep on these unseen software projects. As a baseline, we finetune a model where its training set includes the project, but with non-overlapping instruction pairs ("Regular" in Table 3).

The first two rows in Table 3 demonstrate that NeuDep remains relatively robust when the testing set is collected from unseen projects, *i.e.,* on average, the number of detected dependencies only drops 1.4% and false positives increased by 7%. Interestingly, training without samples from Lynx even increases the detected dependencies, but at the expense of much higher false positives.

Zero-Shot Generalizability to Unseen Optimizations/Obfuscations. Aggressive compiler transformations can bring many challenges to inferring memory dependencies, *e.g.,* substituting instructions introduces more pointer arithmetic operations, which requires reasoning over the bloated instructions to detect the value flows. To study whether NeuDep generalizes to unseen optimizations and obfuscations, we exclude binaries optimized or obfuscated by each strategy (§4) in training and test NeuDep on the excluded binaries.

Table 3 presents results when testing NeuDep on each unseen optimizations and obfuscations. We also include the baseline results when its training set includes those optimized or obfuscated binaries (but with non-overlapping pairs). We observe that NeuDep generalizes to unseen optimizations and obfuscations, with only 2.6% drop in detection rate and 9% increase in false positives.

Runtime Performance. One of the most significant benefits of NeuDep over traditional approaches comes from its speed, as its analysis is amenable to parallelization with GPUs. Table 4 compares the speed of NeuDep to Angr and Ghidra. We run each tool on each project compiled with O0 from our finetuning dataset (§4). We observe that Angr often takes long time and cannot finish running (as also confirmed by [96]). Thus, we time it out after 5 minutes. Consequently, Angr's actual runtime is under-estimated. We do not compare to (i) DeepVSA because it still relies on VSA, so it is at least as slow as any VSA implementation, and (ii) SVF because it works only on LLVM IR, not directly on binaries. Therefore, SVF has extremely high overheard from mapping LLVM IR results to binary. Table 4 shows that NeuDep is 3.5× faster than the second-best tool (Ghidra) and orders of magnitude faster (125.2×) than Angr.

5.2 Ablation Study

We study how much each design in NeuDep (§3) contributes to its performance. We follow the setup in §5.1. Table 5 summarizes the results where we bold NeuDep's default choice.

Pretraining. We first ablate the effectiveness of pretraining in assisting memory dependence analysis. Table 5 shows that pretraining NeuDep significantly improves its performance by 12.6% in the number of detected dependencies. The number of misses and false positives drop by 57.6% and 31.4%, respectively.

Table 5: Ablation on NeuDep designs. We treat the first row of each design as the baseline and compute the improvement of other alternatives.

Ablation Setup		Detect	Miss	FP	Improve (+/-) Detect	Miss	FP
Pretrain	w/o	8,780	1,914	1,477	0.0%	0.0%	0.0%
	w/	**9,882**	**812**	**1,013**	**+12.6%**	**-57.6%**	**-31.4%**
Value Embed	Concat	9,666	1,208	1,027	0.0%	0.0%	0.0%
	Conv.	**9,882**	**812**	**1,013**	**+2.2%**	**-32.8%**	**-1.4%**
Fusing Strategy	Sum	9,752	942	1,419	0.0%	0.0%	0.0%
	1st Layer	**9,882**	**812**	**1,013**	**+1.3%**	**-13.8%**	**-28.6%**
	3rd Layer	9,870	824	1,209	+1.2%	-12.5%	-14.7%
	5th Layer	9,700	994	1,186	+0.5%	-5.5%	-16.4%
Compos. Learning	w/o Compos.	9,806	888	1,389	0.0%	0.0%	0.0%
	w/ Compos.	**9,882**	**812**	**1,013**	**+0.8%**	**-8.6%**	**-27.1%**
Code Addr.	w/o Addr.	9,667	1,027	1,407	0.0%	0.0%	0.0%
	w/ Addr.	**9,882**	**812**	**1,013**	**+2.2%**	**-20.9%**	**-28%**

Byte Aggregation. We study the effectiveness of encoding numeric values using convolutions with highway network (§3.2) by comparing it to the baseline that concatenates the input bytes. Table 5 shows that our encoding mechanism outperforms the baseline by 2.2% and significantly reduces the miss detection rate by 32.8%.

Input Fusion. We explore the effectiveness of input fusion by comparing it to the baseline that takes the vector sum of the input embeddings [64, 66]. We also study fusing after which layer is the most effective. We note that simply summing the embeddings of code and trace values at input by assuming they are homogeneous performs the worst. This confirms our intuition that code and trace are heterogeneous data that benefit from different encoding mechanisms. In addition, we note that combining code and trace at earlier layers performs the best. This is likely because trace values can participate early in the model's computation of interactions between instructions and trace values, *i.e.,* fusing in the later layers implies it has fewer remaining layers to learn how code and trace interacts.

Composition Learning. We study whether composition learning (§2.3) would help the model's finetuning performance for detecting memory dependencies. We compare it to the fixed masking percentage strategy where the samples are shuffled randomly, and the masking rate r is fixed to 0.5 on both the code and trace tokens. Table 5 shows that composition learning moderately improves the model by 0.8% in detected dependencies but substantially reduces the number of false positives by 27.1%. This observation confirms our intuition that arranging the training samples based on their difficulty helps the model learn more efficiently.

Modeling Address Layout. We study whether annotating the binary code with its loaded addresses would bring a useful inductive bias to the model by comparing to the baselines that do not model them [64, 66]. Table 5 shows that annotating the code with addresses significantly reduces the model's missed detection and false positives, *i.e.,* by 20.9% and 28%, respectively. This shows that the code address helps the model reduce the spurious dependencies.

5.3 Performance on Reverse Engineering Tasks

We probe pretrained NeuDep using three reverse engineering tasks that either assist or benefit from memory dependence analysis.

Table 6: Comparison of F1 scores on memory region prediction between NeuDep and PalmTree and other baselines.

	Global	Heap	Stack	Other	Avg.
Instruction2Vec	0.654	0.566	0.914	0.947	0.77
Asm2Vec	0.517	0.359	0.911	0.948	0.684
DeepVSA	0.835	0.584	0.944	0.959	0.831
PalmTree	0.855	0.714	0.95	0.971	0.873
NeuDep	**0.91**	**0.904**	**0.977**	**0.976**	**0.942**

Table 7: We compare NeuDep to EKLAVYA on five function signature tasks across 4 optimizations for caller and callee.

		Caller O0	Caller O1	Caller O2	Caller O3	Callee O0	Callee O1	Callee O2	Callee O3
Ret.	EKLA.	66.62	70.59	73.63	76.19	91.59	88.87	91.92	95.32
	NeuDep	**94.65**	**93.33**	**95.75**	**96.41**	**95.37**	**93.42**	**96.06**	**98.20**
A_1	EKLA.	91.56	90.38	91.21	91.55	95.62	92.40	93.05	92.56
	NeuDep	**97.03**	**97.09**	**98.47**	**99.17**	**97.24**	**95.10**	**97.01**	**97.84**
A_2	EKLA.	81.82	78.70	81.81	82.03	87.25	82.67	82.40	85.07
	NeuDep	**96.08**	**94.86**	**97.68**	**97.51**	**93.30**	**91.34**	**94.66**	**92.45**
A_3	EKLA.	80.28	79.85	81.35	76.63	77.42	69.18	70.93	69.80
	NeuDep	**96.88**	**96.89**	**97.09**	**97.24**	**96.55**	**94.42**	**94.66**	**95.68**
Arity	EKLA.	92.03	86.02	83.80	82.79	97.48	76.24	77.49	78.69
	NeuDep	**98.84**	**95.44**	**96.35**	**95.86**	**99.23**	**92.57**	**95.04**	**96.40**

Memory-Access Regions. We follow PalmTree by running NeuDep on the *DeepVSA's dataset* and compare NeuDep to the reported F1 scores of PalmTree, DeepVSA, and other baselines (§4). We note that DeepVSA's datasets are all 32-bit x86 binaries, but NeuDep is pretrained on x86-64 binaries. However, we find that just our vocabulary constructed from x86-64 binaries covers 89.9% of DeepVSA's dataset vocabulary, likely because both belong to the x86 family. Therefore, we simply apply our vocabulary on DeepVSA's dataset and replace unseen tokens with "unknown" in the vocabulary.

Table 6 shows that NeuDep remains robust across different memory regions. On average, NeuDep outperforms PalmTree by 0.069. On more challenging labels such as heap, NeuDep outperforms PalmTree and DeepVSA by 0.19 and 0.32, respectively. This is likely because accessing these memory regions involves more diverse patterns, *e.g.,* via the stack pointer register (Figure 2).

Function Signature. We compare NeuDep to EKLAVYA on recovering function signatures. Table 7 shows that NeuDep outperforms EKLAVYA on all signature inference tasks, achieving 12.6% higher accuracy on average. Most notably, NeuDep's performance remains robust across different tasks and optimization levels, while EKLAVYA's accuracy shows clear drops. For instance, when comparing the prediction accuracy of 3rd argument (A_3) and 1st argument (A_1), EKLAVYA decreases by 16.61% while NeuDep's drops by only 1.19%. Likewise, within the arity task, EKLAVYA's accuracy decreases 14.02% from O0 to O3, while NeuDep decreases 2.91%.

Indirect Calls. Finally, we compare how well NeuDep, EKLAVYA, and TypeArmor detect indirect calls (Definition 2.4). We consider 8 matching algorithms (§3.6) grouped row-wise by arity matching criteria detailed in Table 8. On all algorithms, NeuDep outperforms EKLAVYA and TypeArmor, achieving 0.032 and 0.07 higher F1 scores, respectively. With loose arity and return type matching –

Table 8: NeuDep's F1 score on matching indirect calls using several heuristic algorithms. TypeArmor cannot infer argument types, so the corresponding cells are dashed out.

		Arity	Arity+Ret	Arity+Arg	Arity+Arg+Ret
Loose	TypeArmor	0.75	0.752	-	-
	EKLAVYA	0.777	0.778	0.8	0.801
	NeuDep	**0.783**	**0.804**	**0.83**	**0.843**
Strict	TypeArmor	0.777	0.778	-	-
	EKLAVYA	0.818	0.817	0.811	0.811
	NeuDep	**0.844**	**0.853**	**0.851**	**0.857**

the criterion adopted in TypeArmor – NeuDep outperforms TypeArmor by 0.052 in F1 score. We also note that NeuDep's performance increases as the matching algorithm incorporates more conditions, while the performance of other systems remains roughly the same.

6 THREATS TO VALIDITY

Architecture Bias. We only consider x86-64 binaries. While we have shown NeuDep generalizes to several x86-32 binaries (§5.3), it cannot directly be applied to binaries with significantly different syntax, *e.g.,* those running on ARM or MIPS architectures. However, as our trace engine supports other architectures well [81], we can potentially pretrain the model for other architectures. We also plan to extend our models to different programming languages that come with efficient tracing support [31, 57, 68].

Performance Bias. We only compare NeuDep's runtime performance on GPUs with other baselines (§5.1), as NeuDep's neural module runs on GPU by default. However, we believe that significantly benefitting from GPU is indeed a key advantage of ML-based techniques over traditional binary analysis that cannot easily exploit GPU parallelism and thus struggle to scale to large binaries.

Ground Truth Bias. Obtaining complete ground truth for memory dependencies in real-world programs is intractable. Therefore, following BDA's approach [96], we resort to dynamic analysis and use the accessed memory locations observed during execution to collect the reference dependencies. While we cannot guarantee the ground truth to be complete, this approach can still quantify how many dependencies are missed by the evaluated tools. Table 2 shows that NeuDep outperforms all baselines with the fewest misses.

Inter-Procedural Analysis. We only capture full execution behavior starting from a callee. Therefore, NeuDep primarily expects instruction pairs to come from the same function. However, as we trace the full execution behavior of method calls, our model potentially learns to reason about the value flows across procedures. We plan to explore NeuDep's capability in inter-procedural analysis by modeling the complete calling context in our future study.

7 RELATED WORK

Binary Memory Dependence Analysis. There has been a long history of efforts to approach the problem of analyzing memory dependencies in executables [5, 6, 11, 16, 22, 34, 35, 71, 96]. Debray *et al.* [22] and Cifuentes *et al.* [16] pioneered this field by using abstract interpretation to propagate the abstract domain along the registers of each instruction. VSA [5] improves on their idea by supporting tracking value flows along both the registers and memory locations. DeepVSA [35] further improves on VSA by learning a neural network to predict the memory-access regions of each instruction to pre-filter those not sharing the regions. BDA [96] uses probabilistic analysis to uniformly sample paths and performs per-path abstract interpretation to avoid precision losses from path merging. While both DeepVSA and BDA sacrifice soundness, they have been shown to significantly assist in debugging crashes [19, 58] and malware analysis. However, they still incur high runtime overhead and produce many false positives for optimized binaries – NeuDep substantially outperforms these tools (§5).

Machine Learning for Program Analysis. Machine learning has shown great promises in analyzing both source code and executables [3, 24, 62, 74] in tasks like type inference [37, 56, 61, 64, 70, 92], code completion [10, 17, 43], program synthesis and generation [79, 88], program repair and fix [2, 26, 41, 80, 97], code summarization [14, 21, 75, 84], general code representation [13, 39, 46, 51, 53, 89], bug/vulnerability detection [23, 48, 63, 73], code clone detection and search [14, 32, 33, 42, 55, 66], code translation [72], comment suggestion [40, 52], and reverse engineering tasks [7, 9, 45, 65]. Recent works have observed that incorporating program behavior is beneficial to learning more effective program representations [45, 60, 63, 64, 66, 89]. For example, Pei *et al.* [64, 66] demonstrate that pretraining ML models with execution traces can help the model understand the program's operational semantics, showing successes in detecting semantically similar binaries and type inference under various code transformations [95]. However, they have no support for data flow through memory and thus do not model fine-grained value flows across memory operations. We show in §5.2 that NeuDep's new designs absent in these works are critical to analyzing memory dependencies.

8 CONCLUSION

We present a new ML-based approach, NeuDep, to predict memory dependencies. We first pretrain NeuDep to understand how instructions propagate dynamic values across memory and registers, then finetune the model to detect memory dependencies statically. We demonstrate that NeuDep is precise and efficient, outperforming the state-of-the-art in both detection accuracy (1.5×) and speed (3.5×). Extensive probing studies demonstrate that NeuDep understands memory access patterns, learns function signatures, and can match indirect calls – these tasks either assist or benefit from inferring memory dependencies. Notably, NeuDep also outperforms the state-of-the-art on these tasks.

ACKNOWLEDGMENTS

We thank the anonymous reviewers for their constructive and valuable feedback. We thank the author of BDA, Zhuo Zhang, for providing valuable insight and suggestion, and running experiments of BDA. This work is sponsored in part by NSF grants CCF-1845893, CCF-2107405, CNS-1564055, and IIS-2221943; ONR grant N00014-17-1-2788; an NSF Career Award; an Accenture Faculty Research Award; a Google Gift; an IBM Faculty Award. Any opinions, findings, conclusions, or recommendations expressed herein are those of the authors, and do not necessarily reflect those of the US Government, NSF, ONR, Accenture, Google, or IBM.

REFERENCES

[1] National Security Agency. 2019. Ghidra Disassembler. https://ghidra-sre.org/.

[2] Miltiadis Allamanis, Earl T Barr, Christian Bird, and Charles Sutton. 2014. Learning natural coding conventions. In *Proceedings of the 22nd ACM SIGSOFT International Symposium on Foundations of Software Engineering*. 281–293.

[3] Miltiadis Allamanis, Earl T Barr, Premkumar Devanbu, and Charles Sutton. 2018. A survey of machine learning for big code and naturalness. *Comput. Surveys* (2018).

[4] Paul-Antoine Arras, Anastasios Andronidis, Luís Pina, Karolis Mituzas, Qianyi Shu, Daniel Grumberg, and Cristian Cadar. 2022. SaBRe: load-time selective binary rewriting. *International Journal on Software Tools for Technology Transfer* (2022), 1–19.

[5] Gogul Balakrishnan and Thomas Reps. 2004. Analyzing memory accesses in x86 executables. In *International conference on compiler construction*.

[6] Gogul Balakrishnan and Thomas Reps. 2010. WYSINWYX: What you see is not what you eXecute. *ACM Transactions on Programming Languages and Systems (TOPLAS)* 32, 6 (2010), 1–84.

[7] Sébastien Bardin, Tristan Benoit, and Jean-Yves Marion. 2021. Compiler and optimization level recognition using graph neural networks. In *MLPA 2020-Machine Learning for Program Analysis*.

[8] Yoshua Bengio, Jérôme Louradour, Ronan Collobert, and Jason Weston. 2009. Curriculum learning. In *Proceedings of the 26th annual international conference on machine learning*. 41–48.

[9] Tristan Benoit, Jean-Yves Marion, and Sébastien Bardin. 2021. Binary level toolchain provenance identification with graph neural networks. In *2021 IEEE International Conference on Software Analysis, Evolution and Reengineering*.

[10] Avishkar Bhoopchand, Tim Rocktäschel, Earl Barr, and Sebastian Riedel. 2016. Learning python code suggestion with a sparse pointer network. *arXiv preprint arXiv:1611.08307* (2016).

[11] David Brumley and James Newsome. 2006. *Alias analysis for assembly*. Technical Report. Technical Report CMU-CS-06-180, Carnegie Mellon University.

[12] Matteo Brunetto, Giovanni Denaro, Leonardo Mariani, and Mauro Pezzè. 2021. On introducing automatic test case generation in practice: A success story and lessons learned. *Journal of Systems and Software* 176 (2021), 110933.

[13] Nghi DQ Bui, Yijun Yu, and Lingxiao Jiang. 2021. Infercode: Self-supervised learning of code representations by predicting subtrees. In *2021 IEEE/ACM 43rd International Conference on Software Engineering (ICSE)*. IEEE, 1186–1197.

[14] Nghi DQ Bui, Yijun Yu, and Lingxiao Jiang. 2021. Self-supervised contrastive learning for code retrieval and summarization via semantic-preserving transformations. In *Proceedings of the 44th International ACM SIGIR Conference on Research and Development in Information Retrieval*. 511–521.

[15] Zheng Leong Chua, Shiqi Shen, Prateek Saxena, and Zhenkai Liang. 2017. Neural nets can learn function type signatures from binaries. In *26th USENIX Security Symposium*.

[16] Cristina Cifuentes and Antoine Fraboulet. 1997. Intraprocedural static slicing of binary executables. In *International Conference on Software Maintenance*.

[17] Matteo Ciniselli, Nathan Cooper, Luca Pascarella, Denys Poshyvanyk, Massimiliano Di Penta, and Gabriele Bavota. 2021. An empirical study on the usage of BERT models for code completion. In *2021 IEEE/ACM 18th International Conference on Mining Software Repositories (MSR)*. IEEE, 108–119.

[18] Marco Cova, Viktoria Felmetsger, Greg Banks, and Giovanni Vigna. 2006. Static detection of vulnerabilities in x86 executables. In *2006 22nd Annual Computer Security Applications Conference (ACSAC'06)*. IEEE, 269–278.

[19] Weidong Cui, Xinyang Ge, Baris Kasikci, Ben Niu, Upamanyu Sharma, Ruoyu Wang, and Insu Yun. 2018. REPT: Reverse debugging of failures in deployed software. In *Operating Systems Design and Implementation*.

[20] Robin David, Sébastien Bardin, Thanh Dinh Ta, Laurent Mounier, Josselin Feist, Marie-Laure Potet, and Jean-Yves Marion. 2016. BINSEC/SE: A dynamic symbolic execution toolkit for binary-level analysis. In *2016 IEEE 23rd International Conference on Software Analysis, Evolution, and Reengineering*.

[21] Yaniv David, Uri Alon, and Eran Yahav. 2020. Neural reverse engineering of stripped binaries using augmented control flow graphs. *Proceedings of the ACM on Programming Languages* 4, OOPSLA (2020), 1–28.

[22] Saumya Debray, Robert Muth, and Matthew Weippert. 1998. Alias analysis of executable code. In *Proceedings of the 25th ACM SIGPLAN-SIGACT symposium on Principles of programming languages*. 12–24.

[23] Renzo Degiovanni and Mike Papadakis. 2022. μBERT: Mutation Testing using Pre-Trained Language Models. *arXiv preprint arXiv:2203.03289* (2022).

[24] Prem Devanbu, Matthew Dwyer, Sebastian Elbaum, Michael Lowry, Kevin Moran, Denys Poshyvanyk, Baishakhi Ray, Rishabh Singh, and Xiangyu Zhang. 2020. Deep learning & software engineering: State of research and future directions. *arXiv preprint arXiv:2009.08525* (2020).

[25] Jacob Devlin, Ming-Wei Chang, Kenton Lee, and Kristina Toutanova. 2019. BERT: Pre-training of deep bidirectional transformers for language understanding. In *2019 Annual Conference of the North American Chapter of the Association for Computational Linguistics: Human Language Technologies*.

[26] Elizabeth Dinella, Todd Mytkowicz, Alexey Svyatkovskiy, Christian Bird, Mayur Naik, and Shuvendu K Lahiri. 2021. Deepmerge: Learning to merge programs. *arXiv preprint arXiv:2105.07569* (2021).

[27] Steven HH Ding, Benjamin CM Fung, and Philippe Charland. 2019. Asm2vec: Boosting static representation robustness for binary clone search against code obfuscation and compiler optimization. In *2019 IEEE Symposium on Security and Privacy (S&P)*. IEEE, 472–489.

[28] Manuel Egele, Maverick Woo, Peter Chapman, and David Brumley. 2014. Blanket execution: Dynamic similarity testing for program binaries and components. In *23rd USENIX Security Symposium (USENIX Security 14)*. 303–317.

[29] Ulfar Erlingsson, Martín Abadi, Michael Vrable, Mihai Budiu, and George C Necula. 2006. XFI: Software guards for system address spaces. In *Proceedings of the 7th symposium on Operating systems design and implementation*. 75–88.

[30] Patrice Godefroid. 2014. Micro execution. In *36th International Conference on Software Engineering*.

[31] Matthias Grimmer, Manuel Rigger, Roland Schatz, Lukas Stadler, and Hanspeter Mössenböck. 2014. Trufflec: Dynamic execution of c on a java virtual machine. In *Proceedings of the 2014 International Conference on Principles and Practices of Programming on the Java platform: Virtual machines, Languages, and Tools*.

[32] Wenchao Gu, Zongjie Li, Cuiyun Gao, Chaozheng Wang, Hongyu Zhang, Zenglin Xu, and Michael R Lyu. 2021. CRaDLe: Deep code retrieval based on semantic dependency learning. *Neural Networks* 141 (2021), 385–394.

[33] Yi Gui, Yao Wan, Hongyu Zhang, Huifang Huang, Yulei Sui, Guandong Xu, Zhiyuan Shao, and Hai Jin. 2022. Cross-Language Binary-Source Code Matching with Intermediate Representations. *arXiv preprint arXiv:2201.07420* (2022).

[34] Bolei Guo, Matthew J Bridges, Spyridon Triantafyllis, Guilherme Ottoni, Easwaran Raman, and David I August. 2005. Practical and accurate low-level pointer analysis. In *International Symposium on Code Generation and Optimization*. IEEE, 291–302.

[35] Wenbo Guo, Dongliang Mu, Xinyu Xing, Min Du, and Dawn Song. 2019. DEEPVSA: Facilitating Value-set Analysis with Deep Learning for Postmortem Program Analysis. In *28th USENIX Security Symposium (USENIX Security 19)*.

[36] Liang He, Hong Hu, Purui Su, and Zhenkai Liang Liang, Yan Cai. 2022. FREEWILL: Automatically Diagnosing Use-after-free Bugs via Reference Miscounting Detection on Binaries. In *USENIX Security Symposium*.

[37] Vincent J Hellendoorn, Christian Bird, Earl T Barr, and Miltiadis Allamanis. 2018. Deep learning type inference. In *European Software Engineering Conference and Symposium on the Foundations of Software Engineering*.

[38] Grant Hernandez, Farhaan Fowze, Dave Tian, Tuba Yavuz, and Kevin RB Butler. 2017. Firmusb: Vetting usb device firmware using domain informed symbolic execution. In *Computer and Communications Security*.

[39] Abram Hindle, Earl T Barr, Mark Gabel, Zhendong Su, and Premkumar Devanbu. 2016. On the naturalness of software. *Commun. ACM* 59, 5 (2016), 122–131.

[40] Yuan Huang, Xinyu Hu, Nan Jia, Xiangping Chen, Yingfei Xiong, and Zibin Zheng. 2019. Learning code context information to predict comment locations. *IEEE Transactions on Reliability* 69, 1 (2019), 88–105.

[41] Faria Huq, Masum Hasan, Md Mahim Anjum Haque, Sazan Mahbub, Anindya Iqbal, and Toufique Ahmed. 2022. Review4Repair: Code review aided automatic program repairing. *Information and Software Technology* 143 (2022), 106765.

[42] Abdullah Al Ishtiaq, Masum Hasan, Md Haque, Mahim Anjum, Kazi Sajeed Mehrab, Tanveer Muttaqueen, Tahmid Hasan, Anindya Iqbal, and Rifat Shahriyar. 2021. BERT2Code: Can Pretrained Language Models be Leveraged for Code Search? *arXiv preprint arXiv:2104.08017* (2021).

[43] Maliheh Izadi, Roberta Gismondi, and Georgios Gousios. 2022. CodeFill: Multi-token Code Completion by Jointly Learning from Structure and Naming Sequences. *arXiv preprint arXiv:2202.06689* (2022).

[44] Ridhi Jain, Rahul Purandare, and Subodh Sharma. 2022. BiRD: Race Detection in Software Binaries under Relaxed Memory Models. *ACM Transactions on Software Engineering and Methodology* (2022).

[45] Xin Jin, Kexin Pei, Jun Yeon Won, and Zhiqiang Lin. 2022. SymLM: Predicting Function Names in Stripped Binaries via Context-Sensitive Execution-Aware Code Embeddings. In *2022 ACM SIGSAC Conference on Computer and Communications Security*.

[46] Geunwoo Kim, Sanghyun Hong, Michael Franz, and Dokyung Song. 2022. Improving cross-platform binary analysis using representation learning via graph alignment. In *Proceedings of the 31st ACM SIGSOFT International Symposium on Software Testing and Analysis*. 151–163.

[47] Sun Hyoung Kim, Cong Sun, Dongrui Zeng, and Gang Tan. 2021. Refining indirect call targets at the binary level. In *Network and Distributed System Security Symposium, NDSS*.

[48] Yunho Kim, Seokhyeon Mun, Shin Yoo, and Moonzoo Kim. 2019. Precise learn-to-rank fault localization using dynamic and static features of target programs. *ACM Transactions on Software Engineering and Methodology* (2019).

[49] JongHyup Lee, Thanassis Avgerinos, and David Brumley. 2011. TIE: Principled reverse engineering of types in binary programs. In *2011 Network and Distributed System Security Symposium*.

[50] Young Jun Lee, Sang-Hoon Choi, Chulwoo Kim, Seung-Ho Lim, and Ki-Woong Park. 2017. Learning binary code with deep learning to detect software weakness.

In *KSII the 9th international conference on internet (ICONI) 2017 symposium*.
[51] Xuezixiang Li, Qu Yu, and Heng Yin. 2021. PalmTree: Learning an Assembly Language Model for Instruction Embedding. In *2021 ACM SIGSAC Conference on Computer and Communications Security*.
[52] Annie Louis, Santanu Kumar Dash, Earl T Barr, Michael D Ernst, and Charles Sutton. 2020. Where should I comment my code? A dataset and model for predicting locations that need comments. In *Proceedings of the 42nd International Conference on Software Engineering: New Ideas and Emerging Results*.
[53] Wei Ma, Mengjie Zhao, Ezekiel Soremekun, Qiang Hu, Jie Zhang, Mike Papadakis, Maxime Cordy, Xiaofei Xie, and Yves Le Traon. 2021. GraphCode2Vec: Generic Code Embedding via Lexical and Program Dependence Analyses. *arXiv preprint arXiv:2112.01218* (2021).
[54] Christopher Manning, Kevin Clark, John Hewitt, Urvashi Khandelwal, and Omer Levy. 2020. Emergent linguistic structure in artificial neural networks trained by self-supervision. *Proceedings of the National Academy of Sciences* (2020).
[55] Nikita Mehrotra, Navdha Agarwal, Piyush Gupta, Saket Anand, David Lo, and Rahul Purandare. 2021. Modeling functional similarity in source code with graph-based Siamese networks. *IEEE Transactions on Software Engineering* (2021).
[56] Amir M Mir, Evaldas Latoskinas, Sebastian Proksch, and Georgios Gousios. 2021. Type4Py: Deep Similarity Learning-Based Type Inference for Python. *arXiv preprint arXiv:2101.04470* (2021).
[57] Shouvick Mondal, Denini Silva, and Marcelo d'Amorim. 2021. Soundy Automated Parallelization of Test Execution. In *2021 IEEE International Conference on Software Maintenance and Evolution (ICSME)*. IEEE, 309–319.
[58] Dongliang Mu, Wenbo Guo, Alejandro Cuevas, Yueqi Chen, Jinxuan Gai, Xinyu Xing, Bing Mao, and Chengyu Song. 2019. RENN: efficient reverse execution with neural-network-assisted alias analysis. In *2019 34th IEEE/ACM International Conference on Automated Software Engineering (ASE)*. 924–935.
[59] Manh-Dung Nguyen, Sébastien Bardin, Richard Bonichon, Roland Groz, and Matthieu Lemerre. 2020. Binary-level Directed Fuzzing for {Use-After-Free} Vulnerabilities. In *23rd International Symposium on Research in Attacks, Intrusions and Defenses (RAID 2020)*. 47–62.
[60] Maxwell Nye, Anders Johan Andreassen, Guy Gur-Ari, Henryk Michalewski, Jacob Austin, David Bieber, David Dohan, Aitor Lewkowycz, Maarten Bosma, David Luan, et al. 2021. Show Your Work: Scratchpads for Intermediate Computation with Language Models. *arXiv preprint arXiv:2112.00114* (2021).
[61] Eirene V Pandi, Earl T Barr, Andrew D Gordon, and Charles Sutton. 2021. Type Inference as Optimization. In *Advances in Programming Languages and Neurosymbolic Systems Workshop*.
[62] Corina S Păsăreanu and Mihaela Bobaru. 2012. Learning techniques for software verification and validation. In *International Symposium On Leveraging Applications of Formal Methods, Verification and Validation*. Springer, 505–507.
[63] Jibesh Patra and Michael Pradel. 2022. Nalin: Learning from Runtime Behavior to Find Name-Value Inconsistencies in Jupyter Notebooks. In *2022 IEEE 31st International Conference on Software Engineering (ICSE)*.
[64] Kexin Pei, Jonas Guan, Matthew Broughton, Zhongtian Chen, Songchen Yao, David Williams-King, Vikas Ummadisetty, Junfeng Yang, Baishakhi Ray, and Suman Jana. 2021. StateFormer: fine-grained type recovery from binaries using generative state modeling. In *Proceedings of the 29th ACM Joint Meeting on European Software Engineering Conference and Symposium on the Foundations of Software Engineering*. 690–702.
[65] Kexin Pei, Jonas Guan, David Williams-King, Junfeng Yang, and Suman Jana. 2021. XDA: Accurate, Robust Disassembly with Transfer Learning. In *2021 Network and Distributed System Security Symposium*.
[66] Kexin Pei, Zhou Xuan, Junfeng Yang, Suman Jana, and Baishakhi Ray. 2021. TREX: Learning Execution Semantics from Micro-Traces for Binary Similarity. In *2021 IEEE Symposium on Security and Privacy*.
[67] Fei Peng, Zhui Deng, Xiangyu Zhang, Dongyan Xu, Zhiqiang Lin, and Zhendong Su. 2014. X-force: Force-executing binary programs for security applications. In *23rd USENIX Security Symposium (USENIX Security 14)*. 829–844.
[68] Luís Pina and Michael Hicks. 2016. Tedsuto: A general framework for testing dynamic software updates. In *2016 IEEE International Conference on Software Testing, Verification and Validation (ICST)*. IEEE, 278–287.
[69] Michael Pradel and Satish Chandra. 2021. Neural software analysis. *Commun. ACM* 65, 1 (2021), 86–96.
[70] Michael Pradel, Georgios Gousios, Jason Liu, and Satish Chandra. 2020. Typewriter: Neural type prediction with search-based validation. In *28th ACM Joint Meeting on European Software Engineering Conference and Symposium on the Foundations of Software Engineering*.
[71] Thomas Reps and Gogul Balakrishnan. 2008. Improved memory-access analysis for x86 executables. In *International Conference on Compiler Construction*.
[72] Baptiste Roziere, Jie M Zhang, Francois Charton, Mark Harman, Gabriel Synnaeve, and Guillaume Lample. 2021. Leveraging Automated Unit Tests for Unsupervised Code Translation. *arXiv preprint arXiv:2110.06773* (2021).
[73] Hendrig Sellik, Onno van Paridon, Georgios Gousios, and Maurício Aniche. 2021. Learning off-by-one mistakes: An empirical study. In *2021 IEEE/ACM 18th International Conference on Mining Software Repositories (MSR)*.
[74] Tushar Sharma, Maria Kechagia, Stefanos Georgiou, Rohit Tiwari, and Federica Sarro. 2021. A Survey on Machine Learning Techniques for Source Code Analysis. *arXiv preprint arXiv:2110.09610* (2021).
[75] Ensheng Shia, Yanlin Wangb, Lun Dub, Junjie Chenc, Shi Hanb, Hongyu Zhangd, Dongmei Zhangb, and Hongbin Suna. 2022. On the Evaluation of Neural Code Summarization. In *2022 International Conference on Software Engineering*.
[76] Rupesh Kumar Srivastava, Klaus Greff, and Jürgen Schmidhuber. 2015. Highway networks. *arXiv preprint arXiv:1505.00387* (2015).
[77] Visual Studio. 2006. x86 Assembly Guide. (2006).
[78] Yulei Sui and Jingling Xue. 2016. SVF: interprocedural static value-flow analysis in LLVM. In *International Conference on Compiler Construction*.
[79] Zeyu Sun, Qihao Zhu, Lili Mou, Yingfei Xiong, Ge Li, and Lu Zhang. 2019. A grammar-based structural cnn decoder for code generation. In *Proceedings of the AAAI conference on artificial intelligence*, Vol. 33. 7055–7062.
[80] Alexey Svyatkovskiy, Todd Mytkowicz, Negar Ghorbani, Sarah Fakhoury, Elizabeth Dinella, Christian Bird, Neel Sundaresan, and Shuvendu Lahiri. 2021. Merge-BERT: Program Merge Conflict Resolution via Neural Transformers. *arXiv preprint arXiv:2109.00084* (2021).
[81] The Qiling Team. 2020. Qiling – A True Instrumentable Binary Emulation Framework. https://qiling.io/.
[82] Victor Van Der Veen, Enes Göktas, Moritz Contag, Andre Pawoloski, Xi Chen, Sanjay Rawat, Herbert Bos, Thorsten Holz, Elias Athanasopoulos, and Cristiano Giuffrida. 2016. A tough call: Mitigating advanced code-reuse attacks at the binary level. In *2016 IEEE Symposium on Security and Privacy*.
[83] Ashish Vaswani, Noam Shazeer, Niki Parmar, Jakob Uszkoreit, Llion Jones, Aidan N Gomez, Łukasz Kaiser, and Illia Polosukhin. 2017. Attention is all you need. In *2017 Advances in Neural Information Processing Systems*.
[84] Chong Wang, Xin Peng, Mingwei Liu, Zhenchang Xing, Xuefang Bai, Bing Xie, and Tuo Wang. 2019. A learning-based approach for automatic construction of domain glossary from source code and documentation. In *Proceedings of the 2019 27th ACM joint meeting on european software engineering conference and symposium on the foundations of software engineering*. 97–108.
[85] Fish Wang and Yan Shoshitaishvili. 2017. Angr-the next generation of binary analysis. In *2017 IEEE Cybersecurity Development*.
[86] Guanhua Wang, Sudipta Chattopadhyay, Ivan Gotovchits, Tulika Mitra, and Abhik Roychoudhury. 2019. oo7: Low-overhead defense against spectre attacks via program analysis. *IEEE Transactions on Software Engineering* (2019).
[87] Haojie Wang, Jidong Zhai, Xiongchao Tang, Bowen Yu, Xiaosong Ma, and Wenguang Chen. 2018. Spindle: Informed Memory Access Monitoring. In *2018 USENIX Annual Technical Conference (USENIX ATC 18)*.
[88] Jingbo Wang, Chungha Sung, Mukund Raghothaman, and Chao Wang. 2021. Data-Driven Synthesis of Provably Sound Side Channel Analyses. *2021 International Conference on Software Engineering* (2021).
[89] Ke Wang and Zhendong Su. 2020. Blended, precise semantic program embeddings. In *Proceedings of the 41st ACM SIGPLAN Conference on Programming Language Design and Implementation*. 121–134.
[90] David Williams-King, Hidenori Kobayashi, Kent Williams-King, Graham Patterson, Frank Spano, Yu Jian Wu, Junfeng Yang, and Vasileios P Kemerlis. 2020. Egalito: Layout-agnostic binary recompilation. In *Proceedings of the Twenty-Fifth International Conference on Architectural Support for Programming Languages and Operating Systems*. 133–147.
[91] Jun Xu, Dongliang Mu, Xinyu Xing, Peng Liu, Ping Chen, and Bing Mao. 2017. Postmortem program analysis with hardware-enhanced post-crash artifacts. In *26th USENIX Security Symposium (USENIX Security 17)*. 17–32.
[92] Zhaogui Xu, Xiangyu Zhang, Lin Chen, Kexin Pei, and Baowen Xu. 2016. Python probabilistic type inference with natural language support. In *24th ACM SIGSOFT international symposium on foundations of software engineering*.
[93] Heng Yin, Dawn Song, Manuel Egele, Christopher Kruegel, and Engin Kirda. 2007. Panorama: capturing system-wide information flow for malware detection and analysis. In *ACM conference on Computer and Communications Security*.
[94] Naville Zhang. 2017. Hikari – an improvement over Obfuscator-LLVM. https://github.com/HikariObfuscator/Hikari.
[95] Weiwei Zhang, Shengjian Guo, Hongyu Zhang, Yulei Sui, Yinxing Xue, and Yun Xu. 2021. Challenging Machine Learning-based Clone Detectors via Semantic-preserving Code Transformations. *arXiv preprint arXiv:2111.10793* (2021).
[96] Zhuo Zhang, Wei You, Guanhong Tao, Guannan Wei, Yonghwi Kwon, and Xiangyu Zhang. 2019. BDA: practical dependence analysis for binary executables by unbiased whole-program path sampling and per-path abstract interpretation. *Proceedings of the ACM on Programming Languages* 3, OOPSLA (2019), 1–31.
[97] Qihao Zhu, Zeyu Sun, Yuan-an Xiao, Wenjie Zhang, Kang Yuan, Yingfei Xiong, and Lu Zhang. 2021. A syntax-guided edit decoder for neural program repair. In *Proceedings of the 29th ACM Joint Meeting on European Software Engineering Conference and Symposium on the Foundations of Software Engineering*.